

Impact of Shared LTE Network High Typical Traffic Loads on Smart Grid Demand Response Schemes

Juho Markkula, Jussi Haapola

Centre for Wireless Communications (CWC)

P.O. Box 4500, FI-900014 University of Oulu, Finland

{juho.markkula, jussi.haapola}@oulu.fi

Abstract—Smart grid (SG) demand response (DR) programs and their management attain higher importance as distributed energy generation becomes more popular in households due to reducing prices of small-scale renewable energy generation equipment. The use of public telecommunications infrastructure is a good candidate for enabling DR communications over SGs, but the LTE networks become excessively congested during peak hours and the SG DR traffic delivery can be degraded. The network simulations evaluate traffic volumes, delivery ratios, and delays of various traffic types, including SG DR communications, when an LTE macrocell network capacity is exceeded by an increased amount of typical traffic types (Skype video call, FTP, Youtube video stream, and HTTP). The results show that the SG DR traffic can be delivered, maintaining satisfactory communications performance also in a highly loaded network conditions. The QoS class of SG DR traffic transmitted in downlink direction can even be considered to be lowered below the QoS of typical traffic types.

I. INTRODUCTION

Advanced metering infrastructure (AMI) is a combination of smart meters, a communication network, and utility systems [1]. The communication network enables two-way communications between the smart meters and the utility system, which contains a metering data management system (MDMS). The main focus of AMI is to provide real-time information and control of household electricity consumption for demand response (DR) applications. A remote terminal unit (RTU), a communication interface connected to a smart meter, transmits information collected by the smart meter to an MDMS that processes it and delivers feedback. For example, a smart meter could provide the current electricity consumption value and an MDMS could specify the electricity price due to the total consumption of multiple smart meters [2], [3], or a system operator could turn on/off each user's device according to a direct load control program that follows the grid state and the defined load shaping policy [4].

In [5], the authors investigated if a public LTE network is suitable for smart grid (SG) automatic meter usage without causing significant hindrance to typical public LTE traffic. Based on the simulation results, regular SG traffic has very little effect on the LTE base station (eNB) or the network load. When considering critical emergency events, such as blackout last gasp messaging, with hundreds of simultaneous packet generations, the network resource allocation capacity was exceeded. Two proposed solutions for mitigating network overloading were effective. The first solution was adding an

artificial, $[0, 1)$ s random delay for packet transmissions. The second solution was applying a hybrid sensor-LTE network where RTUs first transmit data to their cluster head that contains both an IEEE 802.15.4 and an LTE communications interface. Next, the authors have simulated SG DR scenarios in an LTE and a hybrid sensor-LTE network [6]. There were some differences in performance between these two networks. Applying the hybrid sensor-LTE network appeared to have a lower impact on the typical public LTE traffic because the antennas of CLHs were located outside at rooftop height, not inside the houses as RTUs in the LTE network. Previously, the authors have presented a solution to overcome issues relating to lack of LTE base station connectivity for user equipment (UE) considered as RTUs [7]. The solution is an ad hoc mode for the LTE-Advanced UE. The ad hoc mode is applied to reach a relay node that is the nearest UE with base station connection. DR traffic is delivered between clusters of UE and a relay node using multi-hop communications. An uplink scheduling strategy to facilitate the coexistence of smart meters and typical UE in the LTE network is proposed in [8]. The scheduler considers service differentiation, delay constraints, and channel conditions, and it utilizes relays to decrease the number of direct smart meter connections to the eNB. In [9], the LTE network performance is increased by applying a combination of contention and non-contention based random access procedures for smart meters to establish connections and by delivering SG traffic via tracking area update control signaling to conserve resources at the eNB for typical data transmissions. Limitations of signaling constraints in the random access and control channels are explored with LTE access reservation protocol simulations using machine-to-machine (M2M) traffic [10]. A more efficient procedure in case of M2M connection establishment should be considered by taking into account the features of the actual channels.

This paper's contribution is to research the influence of a highly loaded LTE network for the SG DR traffic delivery between 750 RTUs and the SG server. Distinct amounts of typical traffics in a public LTE network are generated by 930 UE to exceed the network capacity, and the effects of quality of service (QoS) class selection for SG DR traffic components are researched. The Riverbed Modeler network simulator is used with detailed physical layer propagation models, detailed LTE functionality, suburban topology, and multiple overlapping applications for SG and public LTE communications.

The paper is organized as follows. In Section II the channel model is described. Section III presents the scenario environment, the key parameters, and the simulation setup for all evaluated cases. The simulation results are presented in Section IV and Section V concludes the paper.

II. DESCRIPTION OF THE CHANNEL MODEL

Communications of the simulation scenario take place in a suburban environment. Outdoor and building entry losses were considered for the channels between the UE/RTUs and the eNB. Outdoor pathloss is the most significant source of attenuation for the signal and it is defined for the LTE channels. Building entry loss is caused by the signal penetration through the building walls [11]. Each wall attenuates the signal by approximately 6 dB causing slow fading [12]. The number of the walls is randomly selected between 0 and 2 causing 0, 6, or 12 dB attenuation for transmitted or received signals for each of the RTUs/UE. This is done to reflect the random positioning of the smart meters (on the side of a building) with respect to the eNB. Modeling fast fading is not necessary due to static devices, i.e., the time variations of the radio channel properties are minimal or very slow [13].

LTE exploits orthogonal frequency division multiplexing (OFDM). Frequency variable channel appears flat over the narrow band of an OFDM subcarrier eliminating the need of complex equalization [14]. Solely narrowband fading occurs, which justifies narrowband radio channel modeling to be applied in evaluation of the LTE channel. In addition to the above-mentioned building entry-loss model, we apply a macrocell pathloss model for suburban environments that is based on the empirical, modified COST231 Hata urban propagation model [15]. The path-loss (PL_H), in dB, is

$$PL_H[dB] = (44.9 - 6.55 \log_{10}(h_{bs})) \log_{10}\left(\frac{d}{1000}\right) + 45.5 + (35.46 - 1.1h_{ms}) \log_{10}(f_c) - 13.82 \log_{10}(h_{bs}) + 0.7h_{ms} + C, \quad (1)$$

where h_{bs} is the LTE-network eNB antenna height in meters, h_{ms} is the UE/RTU antenna height in meters, f_c is the carrier frequency in MHz, d is the distance between eNB and UE/RTU in meters, and $C = 0$ dB is a constant factor for suburban macrocell environment. According to the device heights and the topology presented in the Fig. 1, d varies between 29 and 618 m for UE and RTUs in the LTE network.

III. SCENARIO SETUP

A. Introduction to the Scenario

Fig. 1 presents the simulation topology that is a generalization of a suburban environment, where the gaps between clusters represent discontinuations in houses, like roads, streams, parks, etc. The clusters themselves represent municipal planning of groups of buildings with less order in positioning (random placement of RTUs/UE). The terrain of the suburban region is quite flat and it is divided into 30 clusters, each containing 25 and, in total 750, houses/apartments with DR

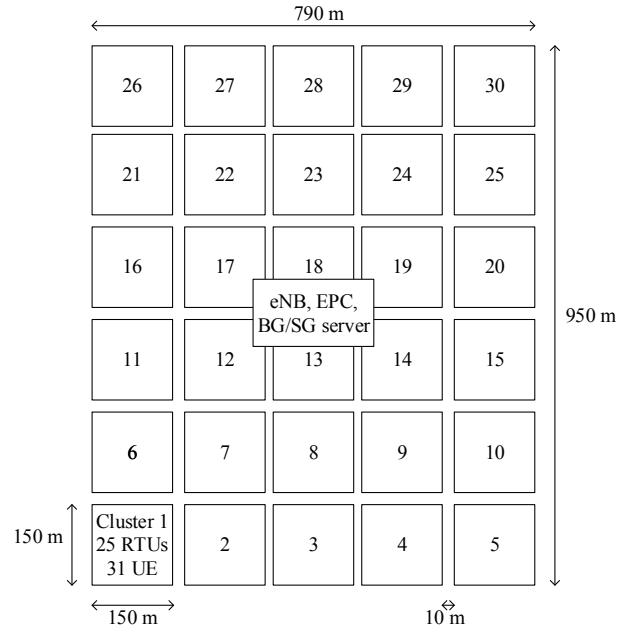


Fig. 1. Evaluated, generalized suburban scenario topology with 750 RTUs and 930 UE. In each cluster the RTUs and UE are randomly positioned.

units, each equipped with RTUs. Every RTU is wirelessly connected with the eNB, and SG server that correspond to the utility system has a wired connection with the evolved packet core (EPC) and the eNB. Smart grid traffic is delivered between the RTUs and the SG server.

It is assumed that an average family size is 3.7 persons and there are three network operators with equal shares of users. Thus, there are in total 930 UE in the area using the same operator as the RTUs, and each cluster contains 31 UE producing typical traffic in the LTE network as background (BG) traffic. A public LTE network of an operator is used for SG traffic without any modifications to typical LTE network configuration. In addition, the simulations are repeated when the QoS of some SG traffic components are kept below the QoS classes of BG traffic components. The RTUs and the UE are randomly (with uniform distribution) positioned inside every cluster at the start of the each simulation run. The purpose of the random placement is to let the DR units to be placed in various locations, not dictated by municipal planning as is usual in real environments. Twenty different setups (each 20 min) that also affect the traffic distributions are averaged per each scenario. In total, 85-95 million data packets were generated in every scenario.

B. Parameters

Key parameters for the LTE network (Table I) are selected by taking into account the simulation topology and the technical specifications [16], [17]. Single input single output (SISO) antenna configuration is applied. Link adaptation and channel dependent scheduling mode signifies that also RTUs/UE will take measurements on various sub-bands and calculate separate modulation and coding scheme (MCS) indexes for

TABLE I
KEY PARAMETERS FOR THE SIMULATION SCENARIOS

LTE parameter	RTU/UE	eNB
Band width	10 MHz (UL)	10 MHz (DL)
Base frequency	1800 MHz	1990 MHz
Transmission power	24 dBm	43 dBm
Tx antenna gain	-0.2 dBi	16.5 dBi
Receiver sensitivity	-106.5 dBm	-120.7 dBm
Antenna height	1.5 m	30 m [SISO]
Cyclic prefix type	7 symbols per slot	
Scheduling mode	Link adaption and channel dependent scheduling	
HARQ retransmissions	Max. 3	
RLC retransmissions	Max. 4 (RTU), 0 (UE)	
PDCP compression ratio	UDP/IP: random [0.5714-0.7143], TCP/IP: random [0.1-0.4], RTP/UDP/IP: random [0.1-0.15]	

each sub-band [14]. The eNB will try to match the RTUs/UE to their preferred sub-bands, perform link adaptation, and create wideband MCS index. Hybrid automatic repeat request (HARQ) retransmission [14] were enabled for all the SG and BG traffics, but radio link control (RLC) retransmissions were solely applied for the SG traffic to improve the packet delivery ratio (PDR). Internet protocol (IP) related headers (IP, UDP, TCP, and RTP) were compressed using packet data convergence protocol (PDCP) [14].

C. Simulation Scenarios

All the scenarios were simulated in an LTE network with exactly the same SG traffic and LTE parameters; only the QoS classes for distinct scenarios and traffic components were varied, and they are defined at the beginning of the Table II. QoS class identifiers (QCIs) number 8 and 9 signify that there is no guaranteed bit-rate (non-GBR) value for the transmitted data, unlike QCIs 1 and 2 have guaranteed bit-rate (GBR) values and lower allocation retention priority (ARP) values admitting a higher priority [18]. The scheduler used in the simulator first allocates bandwidth for the QCIs 1 and 2 with objective to maintain the packet delay budget by using the GBR values. Secondly, the scheduler allocated bandwidth for the QCIs 7 and 8, using an equal capacity algorithm that allows to share the remaining channel capacity equally with traffic queues using the same priority index. The priority indexes for the QCIs 1, 2, 8, and 9 are 0, 2, 2, and 3, respectively, where the smaller number corresponds to the higher priority. The channel bandwidth is served first for the traffic queues with the higher priority index. The traffic of QoS classes (QCI: 1 or 2) that cannot be delivered using GBR, e.g. GBR is not sufficiently high for all the generated traffic, also the equal capacity algorithm is used to allocate bandwidth.

Smart grid traffic is generated as presented in the Table II. Each of the 750 RTUs transmits the instantaneous energy usage updates (one second interval) to the SG server that transmits adjustments at 30 second intervals for every RTU. The frequency of updates enables control of local energy production when the SG server performs adjustments. For example, local renewable energy production, such as solar

power, could be utilized as extra energy during the energy consumption peaks.

1) *QoS case 1*: The QoS case 1 scenario presents simulations when the QoS class (QCI: 9) of SG traffic components is the same as the lowest priority QoS class of BG traffic components (FTP, Youtube video stream, and HTTP). Traffics are generated as presented in the Table II. BG traffic is produced by the UE in uplink (UL) and by the BG server in downlink (DL). BG traffic was modeled as typical busy hour traffic that contains realistically modeled applications. Uplink traffic was about 21% of the total traffic being at the realistic maximum level [19]. The amount of the BG traffic was relatively high because the Skype video call and Youtube video stream were selected to have a high quality, and FTP files, e.g. photos, were also uploaded by the UE. Thus, the purpose was to reach the capacity limits of the network with BG traffic, and to observe the influence of a high loaded LTE network for the SG traffic delivery.

Four scenarios are considered, where all the 930 UE communicate voice over IP traffic and other BG traffics (Skype video call, FTP, Youtube video stream, and HTTP) are generated by 33%, 50%, 67%, and 100% of the UE. In addition, constant amount of SG traffic is generated by the 750 RTUs and the SG server.

2) *QoS case 2*: The QoS case 2 scenario presents simulations when the QoS classes (QCI: 8 or 9) of SG traffic components were at the same or at lower level than the lowest priority QoS class (QCI: 8) of BG traffic components. The intention was to observe the significance of the QoS class selection for the communications performance of the specific SG and BG traffic components. When 33% of the UE were generating also other BG traffic components than voice over IP, the lower priority QoS class (QCI: 9) was selected for the both SG traffic components. For the other BG traffic amounts (50%, 67%, and 100%), the lower priority QoS class (QCI: 9) was selected only for the SG demand response control (DL) traffic component. Other simulation specifications were exactly the same as in the QoS case 1.

IV. SIMULATION RESULTS

The Fig. 2 presents the average application loads for the SG and BG traffics as a function of traffic volume. Overheads of LTE and IP related headers are not included in the loads. The SG traffic in the network is approximately 0.6 Mb/s in UL and 0.02 Mb/s in DL direction. The volume of the BG traffic changes due to the percentage of the UE communicating also Skype video call, FTP, Youtube video stream, and HTTP traffics. In addition, all the UE participate in voice over IP communication. Volume of the BG traffic components was clearly above the SG traffic. The lowest amount of the total traffic (22.65 Mb/s) was generated when 33% of the UE were generating also other BG traffic components than voice over IP, SG and BG (33%), and the highest amount of the total traffic (60.29 Mb/s) was generated when all the UE participated in all the BG traffic applications, SG and BG (100%).

TABLE II
TRAFFIC PARAMETERS OF DISTINCT TRAFFIC COMPONENTS FOR 750 RTUS AND *33%, 50%, 67%, AND 100% OF THE 930 UE.

LTE traffic component	QoS class identifier, ARP		GBR	TLP
SG demand response (UL)	QoS case 1: 9 (non-GBR), 9. QoS case 2: 8 (non-GBR), 8. *9 (non-GBR), 9.		-	UDP
SG demand response control (DL)	9 (non-GBR), 9		-	UDP
Voice over IP	1 (GBR), 2 [Packet delay budget: 100 ms]		96 kb/s	RTP/UDP
Skype video call	2 (GBR), 4 [Packet delay budget: 150 ms]		1.5 Mb/s	UDP
FTP, Youtube video stream, HTTP	QoS case 1: 9 (non-GBR), 9. QoS case 2: 8 (non-GBR), 8.		-	TCP, UDP, TCP
Smart grid traffic per RTU (UL) and Server (DL)	Start time	Generation interval	Payload data	
SG demand response (UL)	random [300-301] s	1 s	800 b	
SG demand response control (DL)	random [300-330] s per each RTU	30 s		
BG traffic per UE in an hour	Start time	Session length/size	Direction (UL/DL)	
Voice over IP (AMR 12.2k)	5 min	2.5 min (silence length: 2 s, talksprout length: random [30-40] s)	50/50%	
Skype video call (640p/30fps)		30 s		
FTP		2 files (23.2 Mb/file)		
Youtube video stream (720p/24fps)		1 min	0/100%	
HTTP		2 pages (24 Mb/page)		
Total BG application traffic		250.9 Mb	21/79%	

The Fig. 3 shows the average application load and throughput values of the total, downlink, and uplink traffics, and the average channel utilization of the physical uplink shared channel (PUSCH) and the physical downlink shared channel (PDSCH) [20] as a function of traffic volume. It can be seen that with the traffic volume: SG and BG (67%), the throughputs (square dotted lines, red) are clearly below the loads (solid lines, blue). The downlink traffic load, generated on an application layer, is approximately 33.14 Mb/s that is about 90% of the total theoretical maximum throughput (36.7 Mb/s) when utilising 50 resource blocks and the highest MCS index number 28 [20]. The average uplink traffic load (9.09 Mb/s) is significantly lower than the the downlink load. The capacity of the UL channel is worse than the DL channel capacity, because lower MCS indexes have to be used due to the limited UE transmission powers. Average channel utilization curves (round dotted lines, green) approach the maximum value (100%), being 98.4% for PUSCH and 87.2% for PDSCH. In addition to the application traffic, transmitting

header and control data consume also the UL and DL channel bandwidths. With the maximum traffic volume: SG and BG (100%), the load is much higher than the throughput and the average channel utilization is 99.3% for PUSCH and 97.8% for PDSCH. Thus, the network capacity is clearly exceeded.

The Fig. 4 shows the average network delays of SG and BG traffic components as a function of traffic volume. Solid lines with blue color represent QoS case 1 and square dotted lines with red color illustrate the results when QoS case 2 parameters (Table II) were used to lower the QoS of some SG traffic components. The peak loads, minimum/maximum/average values of network delays, and the packet delivery ratios (PDRs) over multiple instantiations of the topology are presented in the Table III.

To summarise the Figs. 2, 3, 4, and the Table III, there are no significant differences in communications performance of the BG traffic components when SG traffic was generated using QoS classes according to QoS case 1 or 2. Nevertheless,

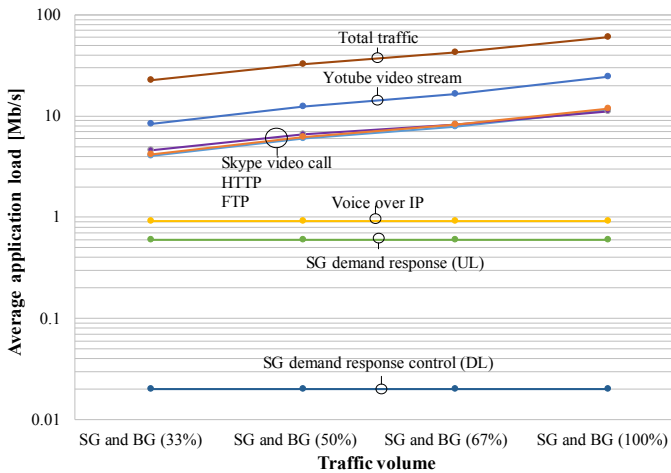


Fig. 2. Average loads of SG and BG traffic components.

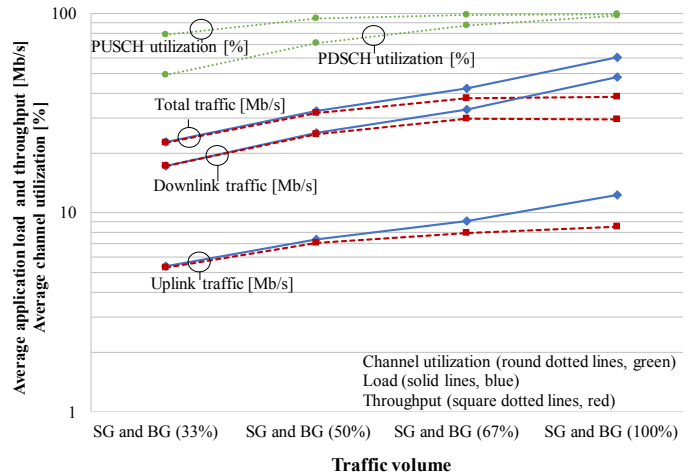


Fig. 3. Average loads and throughputs of total, downlink, and uplink traffics in megabits per second, and average channel utilizations of PUSCH and PDSCH in percentages.

TABLE III

[PEAK LOADS IN MEGABITS PER SECOND], MINIMUM/MAXIMUM/AVERAGE VALUES OF THE NETWORK DELAYS IN SECONDS, AND (PACKET DELIVERY RATIOS IN PERCENTAGES).

Traffic component [peak load]	QoS case	SG and BG (33%) traffic	SG and BG (50%) traffic	SG and BG (67%) traffic	SG and BG (100%) traffic
SG DR (UL) [0.6 Mb/s]	1	0.005/44.64/ 0.142 s (100%)	0.005/80.34/ 0.466 s (100%)	0.005/171.7/ 1.124 s (99.8%)	0.005/273.7/ 3.854 s (99.5%)
	2	0.005/147.69/ 4.391 s (99.1%)	0.005/103.9/ 0.478 s (99.9%)	0.005/176.9/ 1.147 s (99.8%)	0.005/246.38/ 3.837 s (99.5%)
SG DR control (DL) [0.0312 Mb/s]	1	0.001/0.139/ 0.004 s (100%)	0.001/0.14/ 0.004 s (100%)	0.001/0.15/ 0.005 s (100%)	0.001/0.201/ 0.008 s (100%)
	2	0.001/1.803/ 0.068 s (100%)	0.001/2.534/ 0.053 s (100%)	0.001/40.61/ 0.116 s (100%)	0.001/34.38/ 0.249 s (100%)
Voice over IP [1.56, 1.6, 1.73, 1.59 Mb/s]	1	0.082/0.872/ 0.127 s (100%)	0.081/4.898/ 0.128 s (99.9%)	0.081/4.661/ 0.129 s (99.9%)	0.081/3.035/ 0.128 s (100%)
	2	0.081/0.397/ 0.127 s (100%)	0.081/2.849/ 0.127 s (100%)	0.081/5.445/ 0.129 s (99.9%)	0.081/2.333/ 0.127 s (100%)
Skype video call [15.29, 20.39, 20.93, 29.67 Mb/s]	1	0.001/27.76/ 0.099 s (97.9%)	0.001/34.08/ 0.222 s (96.9%)	0.001/35.77/ 0.423 s (96.4%)	0.001/30.29/ 0.838 s (96.9%)
	2	0.001/27.31/ 0.097 s (98%)	0.001/28.68/ 0.231 s (96.9%)	0.001/34.09/ 0.426 s (96.4%)	0.001/35.01/ 0.837 s (96.8%)
FTP (UL) FTP (DL) [69.6, 116, 92.82, 139.2 Mb/s]	1	3.902/353.9/ 30.39 s 3.602/154.9/ 5.858 s (99.7%)	4.06/762.2/ 77.15 s 3.585/642.4/ 17.84 s (93.1%)	3.987/707.3/ 139.3 s 3.613/660.5/ 55 s (74.8%)	4.042/835.8/ 229 s 3.635/880.7/ 168.4 s (36.9%)
	2	3.803/556.5/ 27.59 s 3.603/59.8/ 5.082 s (99.5%)	4.06/781/ 74.939 s 3.597/649.5/ 18.45 s (92.8%)	4.12/800.1/ 141.8 s 3.598/691/ 53.02 s (74.8%)	4.042/778.3/ 231.8 s 3.633/830.4/ 163.2 s (36%)
Yotube video stream [22.4, 30.4, 35.2, 57.6 Mb/s]	1	0.002/25.01/ 0.014 s (100%)	0.002/57.28/ 0.155 s (99.6%)	0.002/57.18/ 0.91 s (94.6%)	0.002/59.81/ 3.549 s (69.3%)
	2	0.002/20.83/ 0.013 s (100%)	0.002/56.38/ 0.148 s (99.6%)	0.002/58.04/ 0.9 s (94.9%)	0.002/59.84/ 3.384 s (70.5%)
HTTP [72, 96, 144, 168 Mb/s]	1	3.722/171.1/ 6.381 s (99.9%)	3.753/688/ 18.62 s (97.1%)	3.772/799.3/ 53.92 s (84.2%)	3.745/857.8/ 167.3 s (40.2%)
	2	3.714/105.5/ 5.583 s (100%)	3.743/608.9/ 17.94 s (96.3%)	3.773/662.7/ 53.94 s (84.6%)	3.774/850.9/ 170.3 s (40.2%)

a slight decrease in the delay of BG traffic components with large files (HTTP and FTP) can be noticed in the QoS case 2 that utilizes the lower QoS for the both SG traffic components (UL and DL), when traffic volume was: SG and BG (33%). However, the PDR decreased (from 100 to 99.1%) and the average delay increased significantly (from 0.142 to 4.391 s) for the SG DR (UL) traffic component in QoS case 2. Thus, with the higher BG traffic volumes (SG and BG (50, 67 and 100%)), the SG DR (UL) traffic was selected to apply the same QoS class as the BG traffic components with the lowest QoS, also in the QoS case 2. With the traffic volumes: SG and BG (50, 67 and 100%), SG DR UL traffic average delay increased with the higher traffic volume, still being on an acceptable level (<3.9 s), and the PDRs were at least 99.5%. SG DR control (DL) traffic is generated more sparsely and transmitted through the DL channel that has a higher capacity than the UL channel. SG DR control (DL) traffic delay was higher in QoS case 2 than in QoS case 1, and the delay increased when the traffic volume was raised. However, the delay was still on a tolerable level (at most 0.249 s) and the PDRs were 100% with all the traffic volumes. The results illustrate that the DR traffic can be delivered also in a highly loaded network when the capacity is exceeded, maintaining satisfactory DR communications performance. SG DR traffic was started randomly and relatively small packets were generated with frequent and periodic intervals. Thus, the

constant traffic characteristics facilitated the scheduling of a sufficient amount of channel capacity for the SG DR traffic.

The delay of the most BG traffic components is observed to have a significant increase when the traffic volume increases. The delay of the voice over IP traffic component stays approximately constant with all the traffic volumes, because it applies the QoS class of highest priority and the volume of the traffic is relatively low. Skype video call application utilizes a QoS class with GBR that is 1.5 Mb/s in UL and in DL (in total 3 Mb/s). However, the generated skype video call traffic amount is above the GBR even with the lowest traffic volume, SG and BG (33%). Thus, the delay increases because channel capacity is scheduled in non-GBR manner for the traffic that cannot be delivered utilizing GBR. The PDRs of the BG traffic components, that used QoS classes without GBR (FTP, Yotube video stream, and HTTP), decreased significantly when the traffic volume was increased to exceed the network capacity. Traffic components utilising QoS classes with GBR (Voice over IP and Skype video call) had their PDRs approximately on a same level with distinct traffic volumes. The maximum delay value presents the delay of a single packet in a highly loaded network with difficult channel conditions caused by the penetration loss through building walls. Thus, the average delay presents a better estimate of the overall application performance.

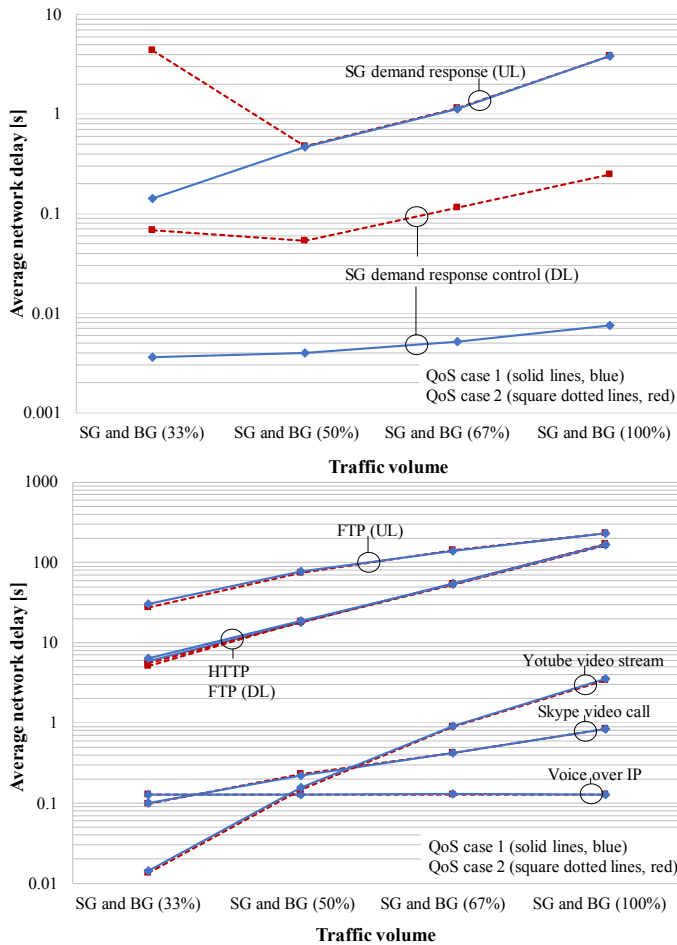


Fig. 4. Average network delays of SG and BG traffic components.

V. CONCLUSION

The paper observed the communications performance when SG DR traffic is transmitted in a highly loaded LTE network. The Riverbed Modeler network simulator was used with detailed physical layer propagation models, detailed LTE functionality, and a suburban topology. Distinct amounts of typical traffics (BG traffics) in a public LTE network were generated and the network capacity was clearly exceeded. The effects of lowering the QoS of some SG DR traffic components, below the QoS classes of typical traffics, were also investigated.

SG DR traffic, with constant traffic characteristics, can be delivered also in a highly loaded network when the capacity is exceeded, maintaining satisfactory DR communications performance. It was not reasonable to lower the QoS of the RTUs that transmitted in UL direction, because the delay increased and the PDR decreased remarkably already with the lowest traffic volume. SG server transmits in DL direction and the QoS could be lowered without significant hindrance for the performance, because the DL channel capacity is remarkably higher than the UL channel capacity. However, lowering QoS of SG DR traffic did not significantly improve typical LTE

traffic performance.

REFERENCES

- [1] V. C. Gungor, D. Sahin, T. Kocak, S. Ergut, C. Buccella, C. Cecati, and G. P. Hancke, *A survey on smart grid potential applications and communication requirements*, IEEE Trans. On Industrial Informatics, vol. 9, no. 1, pp. 28-42, February 2013.
- [2] A.-H. Mohsenian-Rad and A. Leon-Garcia, *Optimal residential load control with price prediction in real-time electricity pricing environments*, IEEE Trans. on Smart Grid, vol. 1, no. 2, pp. 120-133, September 2010.
- [3] C. Ibars, M. Navarro, and L. Giupponi, *Distributed demand management in smart grid with a congestion game*, First IEEE international conference on smart grid communications, pp. 495-500, October 2010.
- [4] A. Molina, A. Gabaldon, J.A. Fuentes, and C. Alvarez, *Implementation and assessment of physically based electrical load models: application to direct load control residential programs*, IEE Proceedings - Generation, Transmission & Distribution, vol. 150, no. 1, pp. 61-66, April 2003.
- [5] J. Markkula and J. Haapola, *Impact of Smart Grid Traffic Peak Loads on Shared LTE Network Performance*, IEEE International Conference on Communications (ICC 2013), June 2013.
- [6] J. Markkula and J. Haapola, *LTE and hybrid sensor-LTE network performances in smart grid demand response scenarios*, IEEE International Conference on Smart Grid Communications, October 2013.
- [7] J. Markkula and J. Haapola, *Ad Hoc LTE Method for Resilient Smart Grid Communications*, Wireless Personal Communications, vol. 98, is. 4, pp. 3355-3375, October 2017.
- [8] M. Carlesso, A. Antonopoulos, F. Granelli, and C. Verikoukis, *Uplink scheduling for smart metering and real-time traffic coexistence in LTE networks*, IEEE International Conference on Communications, pp. 820-825, June 2015.
- [9] C. Karupongsiri, K. S. Munasinghe, and A. Jamalipour, *A novel communication mechanism for Smart Meter packet transmission on LTE networks*, IEEE International Conference on Smart Grid Communications, pp. 122-127, November 2016.
- [10] G. C. Madueño, J. J. Nielsen, D. M. Kim, N. K. Pratas, Č. Stefanović, and P. Popovski, *Assessment of LTE Wireless Access for Monitoring of Energy Distribution in the Smart Grid*, IEEE Journal on Selected Areas in Communications, vol. 34, is. 3, pp. 675-688, February 2016.
- [11] D. Moldkar, *Review on radio propagation into and within buildings*, IEE Proc. on Microwaves, Antennas and Propagation, vol. 138, no. 1, pp. 61-73, February 1991.
- [12] C. R. Anderson and T. S. Rappaport, *In-building wideband partition loss measurements at 2.5 and 60 GHz*, IEEE Trans. On Wireless Communications, vol. 3, no. 3, pp. 922-928, May 2004.
- [13] T.K. Sarkar, Ji Zhong, Kim Kyungjung, A. Medouri and M. Salazar-Palma, *A survey of various propagation models for mobile communication*, IEEE Antennas and Propagation Magazine, vol. 45, no. 3, pp. 51-82, June 2003.
- [14] A. Dahlman, S. Parkvall, J. Sköld and P. Meming, *3G Evolution, HSPA and LTE for Mobile Broadband*, 2nd ed. Oxford, USA: Elsevier Ltd, 2008, pp. 40-46, 105-117, and 131.
- [15] 3GPP, *3rd Generation Partnership Project; Technical Specification Group Radio Access Network; Spatial channel model for Multiple Input Multiple Output (MIMO) simulations [3GPP TR 25.996, Release 10]*, V10.0.0, March 2011, pp. 16-18.
- [16] ETSI, *LTE; Evolved Universal Terrestrial Radio Access (E-UTRA); User Equipment (UE) radio transmission and reception [3GPP TS 36.101, Release 14]*, V14.5.0, November 2017, pp. 115-117, and 285-289.
- [17] ETSI, *LTE; Evolved Universal Terrestrial Radio Access (E-UTRA); Base Station (BS) radio transmission and reception [3GPP TS 36.104, Release 14]*, V14.5.0, October 2017, pp. 50-52, and 111-113.
- [18] 3GPP, *3rd Generation Partnership Project; Technical Specification Group Services and System Aspects; Policy and charging control architecture [3GPP TS 23.203, Release 11]*, V11.5.0, March 2012, pp. 35-38.
- [19] ITU-R, *IMT traffic estimates for the years 2020 to 2030 [Report ITU-R M.2370-0]*, July 2015, pp. 22-29.
- [20] 3GPP, *LTE; Evolved universal terrestrial radio access (E-UTRA); Physical layer procedures; [3GPP TS 36.213, Release 11]*, V11.6.0, March 2014, pp. 29-95, and 100-122.